NeuroImage: Clinical 36 (2022) 103258

Contents lists available at ScienceDirect

NeuroImage: Clinical

journal homepage: www.elsevier.com/locate/ynicl

Neural function underlying reward expectancy and attainment in adolescents with diverse psychiatric symptoms

Qi Liu [a,1], Benjamin A. Ely [a,1], Emily R. Stern [b,c], Junqian Xu [d], Joo-won Kim [d], Danielle G. Pick [a], Carmen M. Alonso [a], Vilma Gabbay [a,b,*]

[a] Department of Psychiatry & Behavioral Science, Albert Einstein College of Medicine, Bronx, NY, United States
[b] Nathan S. Kline Institute for Psychiatric Research, Orangeburg, NY, United States
[c] Department of Psychiatry, New York University School of Medicine, New York, NY, United States
[d] Departments of Radiology and Psychiatry, Baylor College of Medicine, Houston, TX, United States

ARTICLE INFO

Keywords:
Reward expectancy
Reward attainment
Adolescence
fMRI
Depression
Anxiety

ABSTRACT

Reward dysfunction has been hypothesized to play a key role in the development of psychiatric conditions during adolescence. To help capture the complexity of reward function in youth, we used the Reward Flanker fMRI Task, which enabled us to examine neural activity during expectancy and attainment of both certain and uncertain rewards. Participants were 84 psychotropic-medication-free adolescents, including 67 with diverse psychiatric conditions and 17 healthy controls. Functional MRI used high-resolution acquisition and high-fidelity processing techniques modeled after the Human Connectome Project. Analyses examined neural activation during reward expectancy and attainment, and their associations with clinical measures of depression, anxiety, and anhedonia severity, with results controlled for family-wise errors using non-parametric permutation tests. As anticipated, reward expectancy activated regions within the fronto-striatal reward network, thalamus, occipital lobe, superior parietal lobule, temporoparietal junction, and cerebellum. Unexpectedly, however, reward attainment was marked by widespread deactivation in many of these same regions, which we further explored using cosine similarity analysis. Across all subjects, striatum and thalamus activation during reward expectancy negatively correlated with anxiety severity, while activation in numerous cortical and subcortical regions during reward attainment positively correlated with both anxiety and depression severity. These findings highlight the complexity and dynamic nature of neural reward processing in youth.

1. Introduction

Adolescence represents a critical developmental period during which many prodromal psychiatric symptoms and conditions first emerge, including depression, anxiety, and substance abuse (Casey et al., 2010; Fairchild, 2011; Paus, 2005). Adolescence is often defined as a period when reward-seeking behaviors are dominant (Crews et al., 2007; Fairchild, 2011), attributed to rapid maturational changes in cortico-limbic and frontal brain regions central to reward processing. Accordingly, alterations in reward function have been implicated in the emergence of psychiatric conditions in adolescence. While reward function is a complex construct involving multiple temporally distinct processes, there has been sparse research aiming to delineate and distinguish the neural circuitry underlying these distinct reward processes (e.g. anticipation of future rewards, attainment of unexpected rewards) in youth.

To date, most neuroimaging studies of reward function have employed the monetary incentive delay task (MID; Knutson et al., 2000). to examine neural activity during two key reward processes: reward expectancy and reward attainment. In the MID, participants receive cues indicating the monetary value of an upcoming trial, then must respond quickly and accurately in order to receive or avoid losing money. Findings in adolescents based on the MID show that reward expectancy reliably activates the cortical-basal ganglia reward network, while reward attainment increases activity in the ventromedial prefrontal cortex but decrease activity in the thalamus (Cao et al., 2019; Silverman

* Corresponding author at: Department of Psychiatry & Behavioral Science, Albert Einstein College of Medicine, Van Etten Building, 4A-44, 1300 Morris Park Avenue, The Bronx, NY 10461, United States.
E-mail address: vilma.gabbay@einsteinmed.edu (V. Gabbay).
[1] Contributed equally.

https://doi.org/10.1016/j.nicl.2022.103258
Received 5 August 2022; Received in revised form 31 October 2022; Accepted 2 November 2022
Available online 6 November 2022

et al., 2015). To further elucidate the neural underpinnings of distinct reward processes in youth, our group developed the reward flanker task (RFT; Bradley et al., 2017; Stern et al., 2011; Taylor et al., 2006). In addition to trials with certain reward cues where the potential reward value is explicitly indicated, as in the MID, the RFT includes trials with uncertain reward cues, where the monetary reward for a successful response is not known in advance. Distinct from the MID, the RFT also incorporates a challenging conflict discrimination component adapted from the Flanker task, another widely used paradigm (Eriksen and Eriksen, 1974). This cognitive control element is intended to increase task engagement and motivation, enabling us to examine neural mechanisms of reward processing when rewards require effort to earn, as is typically the case for real-life rewards. Due to these advantages, several recent studies by other research groups have adopted the RFT to examine aspects of reward function in clinical cohorts (Costi et al., 2021a; Costi et al., 2021b; Morris et al., 2020). Using the RFT in a pilot sample of 22 clinically heterogeneous adolescents, we found that reward expectancy induced widespread activation, including canonical reward-related regions of the medial frontal cortex and ventral striatum, whereas reward attainment activated memory and emotion-related regions of the medial temporal lobe but did not engage the ventral striatum (Bradley et al., 2017).

The present study expands on this work to examine neural reward processes in a large cohort of adolescents with diverse psychiatric profiles. We utilized an NIMH Research Domain Criteria (RDoC) approach, which recognizes reward dysfunction as a salient feature across psychiatric disorders and addresses the heterogeneous nature of traditional, categorical psychiatric diagnoses. In addition to anhedonia, several studies suggested that reward dysfunction was related to depression and anxiety symptoms either in pediatric or adult population (Ding et al., 2022; Forbes and Dahl, 2012; Sequeira et al., 2022). Considering the high comorbidity between anxiety and depression, we therefore focused on recruiting a diverse sample of psychotropic-medication-free adolescents with a wide range of psychiatric conditions, particularly those with mood and anxiety symptoms but excluding psychosis and substance use, as well as healthy controls (HC). Our analyses examined neural activation to the key processes of reward expectancy and attainment and their associations with dimensional measures of symptom severity across subjects. Secondary analyses further explored the effects of reward magnitude, uncertainty, alternative symptom scales, and group differences between participants with mood and anxiety symptoms vs HCs. Our study utilized a suite of sophisticated fMRI acquisition (Harms et al., 2018), preprocessing (Glasser et al., 2013), denoising (Glasser et al., 2018; Griffanti et al., 2014; Salimi-Khorshidi et al., 2014), and cortical surface alignment (Glasser et al., 2016; Robinson et al., 2014) techniques developed by the Human Connectome Project (HCP). Based on prior findings by our group and others, we hypothesized that: 1) reward expectancy and reward attainment would evoke activation in different regions of the neural reward system; and 2) measures of depression, anhedonia, and anxiety symptom severity would correlate with activation during distinct reward processes and in distinct brain regions across all participants.

2. Methods

2.1. Participants

Participants were recruited from the New York metropolitan area through the Mount Sinai Child and Adolescent Psychiatry Outpatient Clinic, physician referrals, and advertisements in the community. The Institutional Review Boards (IRBs) at Icahn School of Medicine at Mount Sinai and Albert Einstein College of Medicine approved the study, and written informed consent was obtained from participants age 18 and older. Those under the age of 18 provided signed assent, and a parent or legal guardian provided signed informed consent.

2.2. Inclusion and exclusion criteria

As the study utilized an RDoC approach, we sought to recruit a cohort of adolescents with diverse mood and anxiety disorders, including sub-threshold symptoms. Therefore, any adolescents presenting with mood and anxiety symptoms were offered to participate in the study. Based on our prior studies, we expected a wide range of symptom severity in our cohort. In order to capture individuals with low symptom severity, a subset of HC participants was also recruited.

Cohort with psychiatric symptoms: Inclusion criteria: presence of psychiatric symptoms either meeting DSM-IV diagnostic criteria or sub-threshold, based on diagnostic psychiatric assessment (detailed below). Exclusionary criteria: 1) any physical or neurological conditions; 2) estimated IQ < 80, as assessed by the Kaufman Brief Intelligence Test (KBIT; Kaufman, 1990); 3) a positive drug toxicology test on day of scan; 4) a positive pregnancy test on day of scan; 5) current psychosis, pervasive developmental disorder, or substance abuse disorder; 6) psychotropic-medication use in the past 1–3 months at time of visit, depending on drug half-life; 7) any acute illness that might induce inflammation, including the common cold, in the past 2 weeks; and 8) anti-inflammatory medication use, including over-the-counter remedies, in the past 2 weeks.

Healthy controls did not meet criteria for any lifetime psychiatric disorder and were psychotropic-medication-naïve in addition to the exclusionary criteria for psychiatric cohort.

2.3. Clinical assessments

Clinical diagnostic procedures: All participants were assessed using the Schedule for Affective Disorders and Schizophrenia for School-Age Children–Present and Lifetime Version (KSADS-PL; Kaufman et al., 1997). A board-certified child/adolescent psychiatrist or a licensed clinical psychologist trained in administering the KSADS-PL carried out the diagnostic evaluation, with the final clinical report discussed between the Principal Investigator (a licensed child/adolescent psychiatrist) and the assessor.

Overall depression severity was measured by the clinician-rated Children's Depression Rating Scale–Revised (CDRS-R; Poznanski et al., 1985), which was administered to the participant and also a parent/guardian when the participant was under the age of 18. The CDRS-R has 17 items and a score range of 17 to 113.

Anhedonia severity was assessed using the self-rated Temporal Experience of Pleasure Scale (TEPS; Gard et al., 2006), a self-report questionnaire that quantifies both anticipatory (TEPS-AP, score range 10 to 60) and consummatory (TEPS-CP, score range 8 to 48) anhedonia. Unlike other scales used in this study, higher TEPS scores reflect lower levels of anhedonia severity. In addition to the TEPS, two alternative measures were also used to operationalize anhedonia severity for secondary analyses: the Snaith-Hamilton Pleasure Scale (SHAPS; Snaith et al., 1995) and a derived anhedonia score created by combining specific items related to reward function from the clinician-rated CDRS-R and self-rated Beck Depression Inventory Edition (BDI-II; Beck et al., 1996). Details on these alternative measures are provided in the **Supplementary Methods**.

Anxiety severity was assessed using the self-reported Multidimensional Anxiety Scale for Children (MASC; March et al., 1997), which has been validated in both clinical and non-clinical population. This scale contains 39 items and a score range of 0 to 117.

2.4. MRI acquisition

Imaging data were acquired at Mount Sinai's Brain Imaging Center on a 3 T Skyra scanner (Siemens, Germany) with a 16 + 4 channel head + neck coil. Imaging parameters were similar to those used for the HCP LifeSpan protocols (Harms et al., 2018). High resolution (0.9 mm isotropic) T1-weighted anatomical images were acquired using a

MPRAGE sequence with the following parameters: TR / TI / TE = 2400 / 1000 / 2.06 ms, flip angle = 8°, FOV = 256 mm × 256 mm, 224 sagittal slices, 0.9 mm slice thickness (no gaps). Matched 0.9 mm isotropic T2-weighted anatomical images were acquired using a SPACE sequence with the following parameters: TR / TE = 3200 / 566 ms, flip angle = 120°, FOV = 256 mm × 256 mm, 224 sagittal slices, 0.9 mm slice thickness (no gaps). Functional T2*-weighted gradient echo multiband echo planar images (*EPI*) were acquired at 2.3 mm isotropic resolution with alternating LR/RL phase-encoding directions over 4 task runs with the following parameters: TR / TE = 1000 / 31.4 ms, flip angle = 60°, FOV = 624 mm × 720 mm, 60 transverse slices 2.3 mm slice thickness (no gaps), in-plane resolution = 2.3 mm × 2.3 mm, multiband factor = 5, 374 volumes (~6 min) per run. Additionally, a pair of LR-/RL-encoded spin-echo *EPI* fieldmaps with matching parameters was acquired for B_0 field mapping and distortion correction.

2.5. Reward Flanker Task

All participants completed a RFT training session in a mock scanner before the MRI scanning session. During the RFT (Bradley et al., 2017), participants were presented with a monetary cue for 4–6 s then made button presses and earned the cued reward amount if they correctly identified a target letter surrounded by four flanking letters during an allotted response interval, as shown in Fig. 1. Four cues were used: high reward ("50¢"), low reward ("10¢"), no reward ("0¢"), and uncertain reward ("?"). Uncertain reward cues ("?") led to high (50¢), low (10¢) or no (0¢) reward with equal probability. Half of cues were certain and half were uncertain. After the cue, flanker stimuli was presented for 300 ms, followed by a response interval that was calibrated for each participant based on performance during the pre-scan training session (maximum 1700 ms). Participants then received outcome feedback for 2 s informing them of the value of the obtained or unobtained reward. A total of 120 trials were presented in a pseudo-random event-related design over four runs, with 30 trials per run. After each run, participants were told how much money they had earned. Participants were informed of the performance-based bonus prior to RFT in order to increase motivation.

2.6. RFT behavioral data analysis

Reaction times for correct trials and accuracy (percentage of correct responses) were calculated for each of the four cue types (0¢, 10¢, 50¢, and ?) in the four runs combined. Statistical analyses were performed in Matlab 2018b (The MathWorks, Inc.). Separate within-subjects repeated measures ANOVAs were used to assess cue-value effects on reaction time and accuracy. Associations were assessed between reaction time and accuracy with TEPS-AP, TEPS-CP, CDRS-R, and MASC in the whole sample, using Pearson partial correlations controlled for sex and age.

2.7. MRI data pre-processing

MRI analyses followed the HCP minimal preprocessing pipelines (Glasser et al., 2013), including gradient non-linearity and fieldmap-based *EPI* distortion correction, realignment, and normalization to standard Montreal Neurological Institute (MNI) space and 32k CIFTI grayordinate (i.e. cortical surface, subcortical volume) templates. Additionally, we performed two advanced preprocessing steps: denoising via ICA-FIX and multimodal surface alignment via MSMAll. ICA-FIX uses independent components analysis (ICA) and an automated classifier algorithm to identify and remove structured noise components from fMRI data (Griffanti et al., 2014; Salimi-Khorshidi et al., 2014). Specifically, multi-run ICA-FIX (Glasser et al., 2018) was run on the concatenated RFT scans plus a 10 min (600 frame) resting-state fMRI scan collected immediately prior to the RFT. All components identified as "unknown" and "signal" by ICA-FIX were manually reviewed and, where appropriate, reclassified as "noise". All unique variance from the final "noise" components was then regressed out of the concatenated time-series, with all final "signal" and "unknown" components retained. RFT and resting-state runs with excessive motion, defined as more than 3% of frames with relative motion greater than 1 mm, were excluded from ICA-FIX and further analyses. To improve inter-subject cortical alignment,

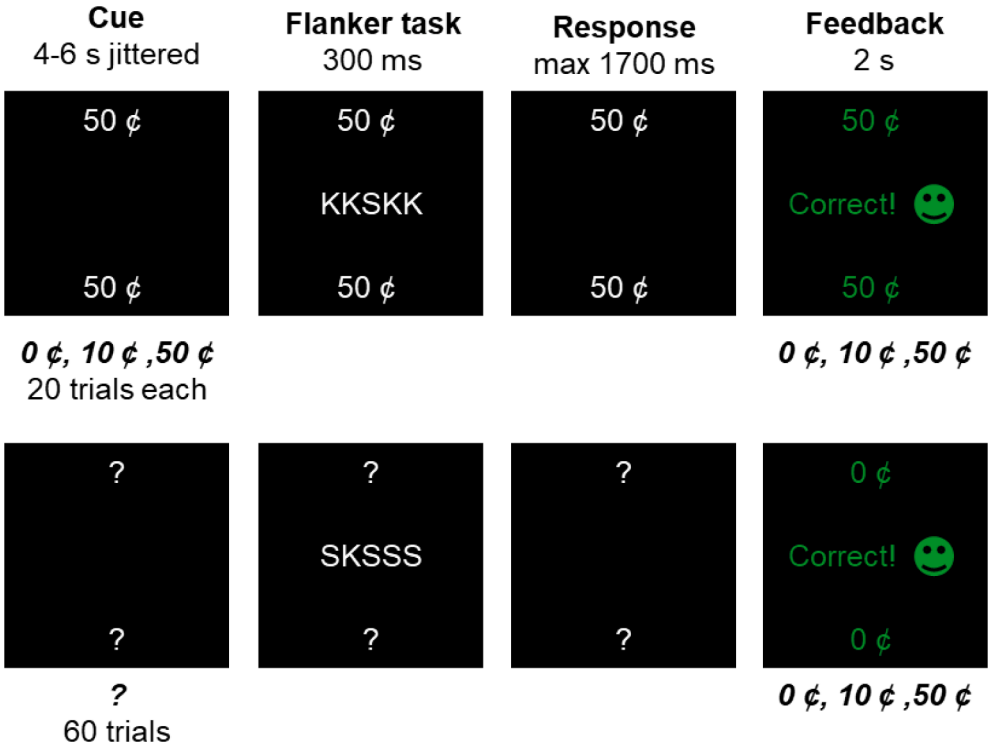

Fig. 1. Reward Flanker Task (RFT) includes: 1) Cues indicating high (50¢), low (10¢), no (0¢), or uncertain (?) reward value; 2) Flanker stimulus; 3) Calibrated window to respond to flanker stimulus.;4) Reward or non-reward feedback.

we further performed multimodal surface matching (MSMAll), which uses a combination of cortical folding, myelination, and fMRI network features to robustly identify corresponding cortical areas even between subjects with divergent cortical folding patterns (Glasser et al., 2016; Robinson et al., 2014). As illustrated in **Fig. S1**, both ICA-FIX and MSMAll improved data quality, yielding group-level activation maps with more focused activation and clearer boundaries compared to analyses conducted without these steps.

2.8. fMRI analysis

Subject-level analyses were performed in Statistical Parametric Mapping (SPM) version 12 (Wellcome Trust Centre for Neuroimaging, London, UK) running on Matlab 2018b. Preprocessed fMRI data were spatially smoothed (4 mm FWHM) in CIFTI space and converted to SPM-supported NIFTI format via Connectome Workbench version 3.2.7 (Glasser et al., 2013). Eleven task-based regressors were specified: four for cues (high-, low-, non–, and uncertain-reward cues), six for feedback (high-, low-, and non-reward feedback on correct trials, separately for certain and uncertain cues), and one for error feedback (incorrect trials, if applicable). Each regressor was convolved with a canonical hemodynamic response function using the general linear model (GLM). Runs with empty feedback regressors were also eliminated from further analyses. Subjects were excluded if more than 25% of RFT data (greater than 1 of 4 runs) were unusable.

Two main subject-level contrasts were examined. Reward expectancy was defined as neural activation during reward cues (10¢ + 50¢) versus non-reward cues (0¢). This contrast measures the differential activation during intervals when participants have been told they can earn a reward relative to intervals when they have been told no reward can be earned, thus capturing the unique neural representation of reward expectancy. Reward attainment was defined as neural activation while receiving reward (10¢ + 50¢) versus non-reward (0¢) outcomes for both certain and uncertain cues. This contrast measures the differential activation during trial feedback that includes a monetary reward relative to trial feedback that does not include a monetary reward, thus capturing the unique neural representation of reward attainment. Secondary contrasts examined activation to reward expectancy and attainment between different reward magnitudes and separately examined activation to reward attainment following only certain cues and only uncertain cues (see **Supplementary Methods**). All resulting subject-level contrast maps were converted back to CIFTI space for group analyses.

Primary group-level analyses examined mean activation to reward expectancy and reward attainment as well as their associations with clinical symptom scales across all subjects. Correlation analyses were performed for measures of depression (CDRS-R), anticipatory anhedonia (TEPS-AP), consummatory anhedonia (TEPS-CP), and anxiety (MASC) severity in the full sample. Secondary analyses reported in the **Supplementary Material** explored: 1) group differences in activation between adolescents with mood and anxiety symptoms vs HC; 2) effects of reward magnitude on activation to reward expectancy and attainment; 3) mean activation during certain and uncertain reward attainment contrasts; and 4) correlations with alternative anhedonia measures. Since many regions showed activation during reward expectancy but deactivation during reward attainment, additional *post hoc* analyses used cosine similarity to quantify these opposite activation patterns, also described in the **Supplementary Material**. All analyses included sex and age as covariates of no interest.

Group-level analyses were performed in FSL PALM (Winkler et al., 2014) using Threshold-Free Cluster Enhancement (TFCE) and non-parametric permutation and sign-flipping tests to control the family-wise error (FWE) rate. These statistical approaches are increasingly advocated by biostatisticians in the field due to their precise Type 1 error control and robustness to skewed or otherwise non-normal data distributions (Cox et al., 2017a; Cox et al., 2017b; Eklund et al., 2016; Winkler et al., 2016). Importantly, our task data were obtained using multiband fMRI sequences with high spatial and temporal resolution and were denoised using an ICA-FIX classifier, ensuring the validity of inferences from one-sample tests conducted via sign-flipping (Eklund et al., 2019). Due to the spatial dependence of TFCE and the discrete representation of major brain structures in CIFTI space, analyses were performed separately for cortical surfaces and for the bilateral subcortical volume, then merged. Results for main analyses were considered significant at the two-tailed $p_{TFCE\text{-}FWE} < 0.05$ level across the whole brain, with each analysis treated as independent. To help discriminate peaks within large activation clusters, results are also presented in the **Supplementary Material** at the more stringent $p_{TFCE\text{-}FWE} < 0.005$ threshold. Information on significant clusters was reported based on the *ciftify_statclust_report* function, as implemented in Ciftify (Dickie et al., 2019). Data and group-level results are available upon request from the authors.

3. Results

3.1. Participants

Participants consisted of 84 adolescents (age, M ± SD: 15.3 ± 2.14; range: 12–20 years; 52 female), of whom 59 presented with diverse mood and/or anxiety symptoms, 8 presented with externalizing disorders such as ADHD and ODD but without mood or anxiety symptoms, and 17 were HC with no significant clinical presentation or history of psychiatric symptomatology. Data from 20 adolescents (age, M ± SD: 15.8 ± 2.38, range: 12–20 years; 9 female) were previously reported as part of an earlier pilot RFT study (Bradley et al., 2017). Clinical and demographic data from participants are compiled in Table 1. As noted in the **Methods**, all participants were psychotropic-medication-free and had at least 3 usable RFT fMRI runs as well as useable anatomical MRI data. **Fig.S2** show the distribution of clinical assessment scores. No relationship was found between age and any clinical symptom scale (all $|r| < 0.12$ and $p > 0.33$).

3.2. RFT behavioral performance during fMRI scan

For RFT, overall task accuracy (percent correct, $M \pm SD$) was 86.63% ± 9.14%, with only 4.07% ± 3.83% of trials omitted (i.e. no response). There was significant difference ($F_{(3,249)} = 4.01$, $p = 0.008$) in accuracy between cue types (0¢: 85.46% ± 12.61%; 10¢: 84.76% ± 11.03%; 50¢: 87.76% ± 10.65%; ?: 87.26% ± 9.36%). Follow-up pairwise comparisons showed that accuracy significantly increased from 10¢ to 50¢ cues ($p = 0.02$), with a trend-level increase from 10¢ to ? cues ($p = 0.06$). Consummatory anhedonia (TEPS-CP) severity was correlated with task accuracy after 0¢ cues ($\rho = 0.29$, $p = 0.01$), 50¢ cues ($\rho = 0.31$, $p = 0.01$), and ? cues ($\rho = 0.24$, $p = 0.049$), indicating better flanker task performance in youth experiencing less anhedonia. No other significant associations with clinical measures were found.

Overall reaction time (M ± SD) was 692.75 ± 115.90 ms. There was significant difference ($F_{(3,249)} = 3.10$, $p = 0.02$) in reaction time between cue types (0¢: 693.70 ± 122.01 ms; 10¢: 681.66 ± 118.22 ms; 50¢: 681.84 ± 141.51 ms; ?: 697.88 ± 118.63 ms). Follow-up pairwise comparisons indicated a trend-level increase in reaction time after ? cues relative to 10¢ cues ($p = 0.07$) and 50¢ cues ($p = 0.08$). The only significant association between reaction time and clinical measures was with the MASC after 10¢ cues ($\rho = 0.23$, $p = 0.048$).

3.3. Neural activation during reward processes

Maps showing significant (two-tailed $p_{TFCE\text{-}FWE} < 0.05$) neural activation/deactivation during reward expectancy and reward attainment are displayed in Fig. 2**a-b**. To avoid ambiguity from the overlap of spatially extended activation clusters, cortical sub-peaks were identified as the upper and lower 5% of activation magnitudes for significant vertices in a given contrast. Table 2 provides detailed information on all

Table 1
Demographic and clinical characteristics.

Whole Cohort Demographics (N = 84)			
Age (Years)	**15.3 ± 2.14 (12–20)**	**Ethnicity (Caucasian/ African American/ Other)**	**39/28/17 (46.43/33.33/ 20.24)**
Sex (F/M)	52/32 (61.9/ 38.1)		
Psychiatric cohort	67(79.76)	HC	17 (20.24)
Psychiatric Cohort Diagnoses (Current/Past) (n = 67)			
MDD	30/5 (44.78/ 7.46)	Other Mood Disorder	3/2 (4.48/2.99)
Dysthymia	4/0 (5.97/0)	OCD	2/1 (2.99/1.49)
DDNOS	3/0 (4.48/0)	ODD	7/0 (10.45/0)
Bipolar Disorder II	3/0 (4.48/0)	ADHD	21/1 (31.34/ 1.49)
Anxiety	42/1 (62.69/ 1.49)	Other	5/2 (7.46/2.99)
Med-naïve/ Med-free	56/11 (83.58/ 16.42)		
Whole Cohort Clinical Assessments			
TEPS-AP [e]	46.89 ± 8.05 (20–60)	CDRS-R [a]	31.93 ± 14.6 (17–78)
TEPS-CP [e]	34.22 ± 7.93 (11–48)	MASC [c]	41.49 ± 17.14 (2–87)
Mood and Anxiety Subgroup Demographics (n = 59)			
Age (Years)	15.25 ± 2.14 (12–20)	Ethnicity (Caucasian/ African American/Other)	30/16/13 (50.85/ 27.12/22.03)
Sex (F/M)	41/18 (69.49/ 30.51)		
Mood and Anxiety Subgroup Clinical Assessments			
TEPS-AP [d]	45.18 ± 8.10 (20–60)	CDRS-R [a]	37.09 ± 14.55 (17–78)
TEPS-CP [d]	33.18 ± 7.37 (14–48)	MASC	44.80 ± 16.55 (11–87)
HC Subgroup Demographics (n = 17)			
Age (Years)	15.65 ± 2.47 (12–20)	Ethnicity (Caucasian/ African American/Other)	6/7/4 (35.29/ 41.18/23.53)
Sex (F/M)	6/11(35.29/ 64.71)		
HC Subgroup Clinical Assessments			
TEPS-AP	49.88 ± 7.00 (33–58)	CDRS-R	18.29 ± 1.53 (17–22)
TEPS-CP	36.06 ± 9.72 (11–48)	MASC [b]	26.43 ± 12.47 (2–49)

Note: Values reported as M ± SD (Range) or n (%), as appropriate. Diagnoses and assessments were based on the DSM-IV to keep consistency across all participants over time. As participants could meet full or subthreshold criteria for more than one disorder, totals may not sum to 100%. MDD: major depressive disorder; DDNOS: depressive disorder not otherwise specified; Anxiety: includes generalized anxiety, social anxiety, phobia, post-traumatic stress, panic disorders, and anxiety disorder not otherwise specified; OCD: obsessive–compulsive disorder; ODD: oppositional defiant disorder; ADHD: attention-deficit/ hyperactivity disorder; HC: healthy controls with no history of psychiatric illness. TEPS-AP/-CP: Temporal Experience of Pleasure Scale, Anticipatory/ Consummatory Pleasure subscales; CDRS-R: Children's Depression Rating Scale-Revised; MASC: Multidimensional Anxiety Scale for Children. Data missing for: [a] 1 participant; [b] 3 participants; [c] 4 participants; [d] 9 participants; [e] 12 participants.

subcortical clusters larger than 40 mm^3 and 10 largest cortical sub-peaks which are larger than 40 mm^2. As there is currently no standard approach for reporting locations on the cortical surface, Table 2 includes the largest overlap with three widely used cortical atlases—the Desikan-Killiany atlas implemented in Freesurfer (Desikan et al., 2006), HCP multimodal parcellation (MMP) atlas (Glasser et al., 2016), and 7-network intrinsic functional connectivity (iFC) atlas (Yeo et al., 2011)—to help characterize cortical sub-peak locations and interpret their possible functions. Group-level result maps in CIFTI format are available upon request.

Reward expectancy (Fig. 2**a**): The contrast of reward cues vs non-reward cues activated the cortical-basal ganglia reward network, including bilateral dorsal anterior cingulate cortex (dACC), mid-cingulate cortex (MCC), insula, striatum, and thalamus. In addition, reward expectancy activated the dorsal lateral prefrontal cortex (dlPFC), inferior frontal gyrus (IFG), inferior and middle occipital lobe, superior parietal lobule (SPL), temporo-parietal junction (TPJ), and cerebellum. Results are also displayed at a more conservative threshold ($p_{TFCE\text{-}FWE} < 0.005$) in **Supplementary Fig. S3**.

Reward attainment (Fig. 2**b**): The contrast of reward feedback vs non-reward feedback only activated the left occipital pole. However, numerous brain regions that were activated by reward expectancy were deactivated during reward attainment, including the bilateral dACC, MCC, lateral occipital lobe (LOC), SPL, TPJ, insula, IFG, thalamus, and cerebellum. Results are also displayed at a more conservative threshold ($p_{TFCE\text{-}FWE} < 0.005$) in **Supplementary Fig. S3**.

3.4. Associations between clinical assessments and neural reward activation

Significant correlations between neural reward processes and dimensional symptom scales are presented in Fig. 3 and detailed in Table 3 (limited to subcortical clusters greater than 40 mm^3 and 10 largest cortical sub-peaks greater than 40 mm^2 in the top/bottom 5th percentile of activation magnitude, as in Table 2).

Depression severity (Fig. 3**a**): Depression scores (CDRS-R) positively correlated with neural activation during reward attainment in a wide range of brain areas, including the bilateral dACC, MCC, PCC, LOC, SPL, TPJ, insula, IFG, somatomotor strip, thalamus, striatum, and cerebellum. No relationship was found with reward expectancy. Results are also displayed at a more conservative threshold ($p_{TFCE\text{-}FWE} < 0.005$) in **Supplementary Fig. S4**.

Anhedonia severity: No significant associations with reward expectancy or attainment were found with either anticipatory anhedonia (TEPS-AP) or consummatory anhedonia (TEPS-CP).

Anxiety severity (Fig. 3**b-c**): Anxiety scores (MASC) were also positively correlated with neural activation during reward attainment in the bilateral dACC, MCC, PCC, LOC, SPL, TPJ, insula, IFG, somatomotor strip, thalamus, and cerebellum. Unlike other symptoms, anxiety was also negatively correlated with activation during reward expectancy in the bilateral thalamus and striatum, including discrete clusters in the caudate, putamen, and nucleus accumbens. Results are also displayed at a more conservative threshold ($p_{TFCE\text{-}FWE} < 0.005$) in **Supplementary Fig. S3**.

3.5. Secondary analyses

In addition to the primary findings detailed above, results from several secondary analyses are reported in our **Supplementary Material** and described here briefly:

Reward magnitude: Contrasts were created to compare high-reward (50¢) vs non-reward (0¢), low-reward (10¢) vs non-reward (0¢), and high-reward (50¢) vs low-reward (0¢), examined separately for cues (reward expectancy) and outcomes (reward attainment). Unthresholded reward expectancy and attainment magnitude contrasts (**Fig. S5**) strongly resembled the respective contrast maps from the main analysis but with reduced *t*-values, suggesting a role of reward magnitude. However, differences between high-reward and low-reward attainment were minimal; only two small clusters in the occipital lobe met significance, supporting our decision to collapse these contrasts in our main analysis.

Reward attainment after certain and uncertain cues: In both cases, unthresholded whole-brain activation patterns (**Fig. S6**) were again highly similar to the main reward attainment contrast. Notably, however, reward attainment after uncertain cues significantly activated the left nucleus accumbens in addition to the occipital pole (**Fig. S7**).

Reward activation in adolescents with mood and anxiety symptoms

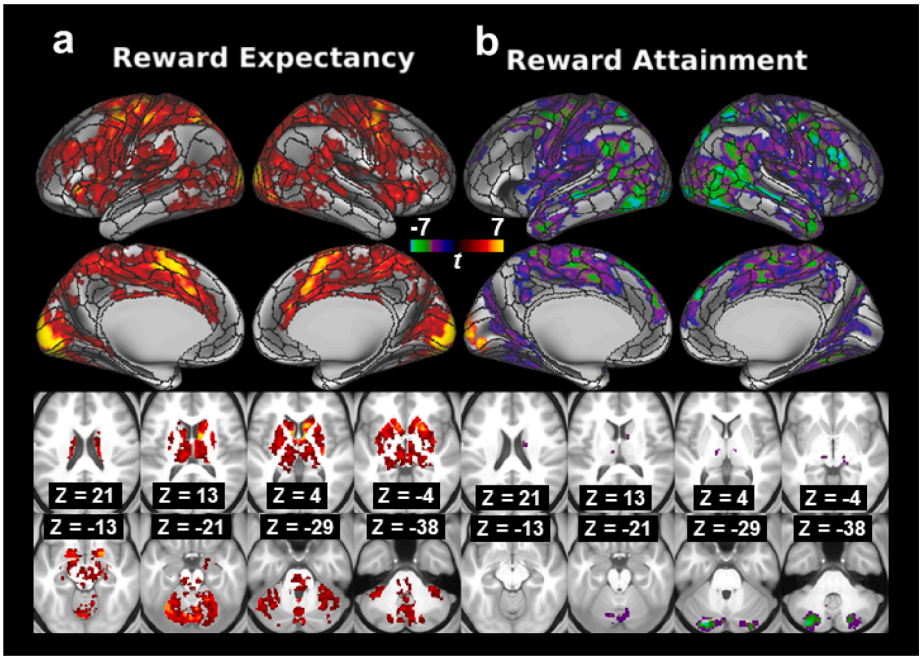

Fig. 2. Neural activation maps ($p_{TFCE\text{-}FWE} < 0.05$) during a) reward expectancy (reward vs. non-reward cues) and b) reward attainment (reward vs non-reward outcomes after both certain and uncertain cues). The background overlay is sulcus depth averaged from HCP 1200 subjects dataset. Black lines on the surface represent HCP MMP Atlas (Glasser et al., 2016).

vs HC: Relative to HC, adolescents with mood and anxiety symptoms exhibited weaker activation in the bilateral thalamus and right caudate during reward expectancy but stronger activation in the bilateral visual cortex during reward attainment (Fig. S8).

Associations between reward activation and alternative anhedonia scales: As in our main analysis using the TEPS, no associations were detected between the SHAPS and neural activation during reward expectancy or attainment. However, derived anhedonia scores were associated with a widespread pattern of neural activation during reward attainment (Fig. S9). This pattern strongly resembled the corresponding association with overall depression severity (CDRS-R) in the main analysis (Fig. 3**a**), and the derived anhedonia score correlations did not remain significant after controlling for depression severity.

Activation during reward expectancy versus attainment: As shown in Fig. 2**a-b**, many brain regions that were activated during reward expectancy had suppressed activity during reward attainment. *Post hoc* analyses revealed that the cosine similarity coefficient between reward expectancy and attainment contrasts was significantly negative only for certain reward attainment (Fig. S10). Follow-up analyses indicated that cosine similarity between reward expectancy and certain reward attainment contrasts was less negative for the mood and anxiety subgroup vs healthy controls (Fig. S11), and that less negative cosine similarity between these contrasts was associated with higher depression scores (Fig. S12).

4. Discussion

The present study examined brain function using the Reward Flanker Task to identify distinct neural processes during reward expectancy and reward attainment in a group of adolescents with diverse psychiatric profiles and HC. As hypothesized, reward expectancy activated the cortical-basal ganglia reward network. Unexpectedly, however, a large range of cortical regions and subcortical areas were more activated during non-reward attainment than reward attainment. Additionally, activation during these reward processes was associated with symptom severity across subjects.

This study was designed to address persistent gaps in the understanding of reward function and its relationship to underlying neural circuitry in youth, which has important implications for the study of adolescent mood disorders. Of particular theoretical interest is anhedonia, which can be readily defined clinically as "the decreased capacity to experience pleasure". Neurobiologically, however, the capacity to experience pleasure is a highly complex phenomenon emerging from the interaction of multiple neural systems over time. Consequently, disturbances in neural circuits subserving different aspects of reward processing may result in similar impairments in overall reward function that are nevertheless etiologically distinct. For example, one individual may have deficits in motivation to obtain a reward while another may be unable to enjoy a reward once obtained, respectively corresponding to impairments in reward expectancy and reward attainment. In both cases, these individuals might be less inclined to seek out pleasurable activities and be diagnosed with "anhedonia" despite the substantially different root causes of their clinical presentations. This concern is even more relevant to clinically heterogeneous phenomena such as overall depression and anxiety severity, which ostensibly reflect multiple cumulative alterations both within and beyond the reward circuitry.

Based on this conceptual model of adolescent psychopathology, our team has developed the Reward Flanker Task specifically to delineate the neural circuitry underlying distinct, yet complementary, reward processes. The task includes uncertain as well as certain cues and allows for the assessment of brain function during both reward expectancy and reward attainment processes, as well as for the separation of reward attainment under certain versus uncertain conditions. Compared with our prior pilot study (Bradley et al., 2017), which examined the different neural responses to reward expectancy and attainment after certain cues, the current study included non-reward expectation and receipt to control shared cognitive components (Liu et al., 2020). In addition, the current analyses examined activation during reward attainment after certain and uncertain cues separately, which examined the neural responses during attainment with different expectation.

Our finding that reward expectancy activated the cortical-basal ganglia reward system, including core ventral striatum and medial frontal cortex regions, is in agreement with previous results in both adult and pediatric populations (Haber and Knutson, 2010; Wang et al.,

Table 2
Neural reward activation during reward expectancy and attainment.

Side	Peak *T*	Area (mm^2)		*Reward Expectancy (RE)*[a] Cluster Overlap		
			Desikan-Killiany Atlas (Desikan 2006)	**HCP Atlas (Glasser 2016)**	**7-Network iFC Atlas (Yeo 2011)**	
Left	14.4	4885	Lateral Occipital (51.9 %)	V1 (29 %)	Visual (100 %)	
Right	13.9	3796	Lateral Occipital (57.8 %)	V1 (31.2 %)	Visual (100 %)	
Right	6.9	881	Superior Frontal (95.2 %)	SCEF (44 %)	Ventral Attention (98.4 %)	
Left	7.0	813	Pre-central (62.9 %)	FEF (48.3 %)	Dorsal Attention (73.4 %)	
Left	8.8	811	Superior Frontal (100 %)	SCEF (64.4 %)	Ventral Attention (65.1 %)	
Right	7.8	723	Pre-central (64.3 %)	6a (49.4 %)	Dorsal Attention (70.2 %)	
Left	7.0	609	Pre-central (100 %)	4 (60.8 %)	Somatomotor (100 %)	
Left	6.6	579	Post-central (100 %)	3b (56.5 %)	Somatomotor (100 %)	
Left	6.5	418	Superior Parietal (87.8 %)	LIPd (43.9 %)	Dorsal Attention (59.7 %)	
Right	6.2	191	Rostral Middle Frontal (100 %)	46 (83.9 %)	Ventral Attention (70.5 %)	
Side	**Peak *T***	**Vol.**(mm^3)		**Peak Coordinates (MNI)**		**Brain Region**
			X	**Y**	**Z**	
Left	7.7	128,816	−30	−66	−54	Striatum; Thalamus;
Right	7.2		10	2	10	Cerebellum
Right	6.9		10	16	4	
				Reward Attainment (RA) [b]		
Side	**Peak *T***	**Area (mm^2)**		**Cluster Overlap**		
			Desikan-Killiany Atlas (Desikan 2006)	**HCP Atlas (Glasser 2016)**	**7-Network iFC Atlas (Yeo 2011)**	
Left	8.0	2294	Lateral Occipital (46 %)	V1 (42.4 %)	Visual (100 %)	
Right	−8.6	3341	Middle Temporal (24.3 %)	TPOJ1 (14.9 %)	Default (32.2 %)	
Left	−8.7	1026	Fusiform (41.9 %)	PH (58.2 %)	Dorsal Attention (69.4 %)	
Left	−8.9	908	Lateral Occipital (100 %)	V1 (36.1 %)	Visual (100 %)	
Right	−10.4	732	Pars-opercularis (62.4 %)	IFSp (46.1 %)	Frontoparietal (88.1 %)	
Right	−8.0	712	Lateral Occipital (100 %)	V3 (33.1 %)	Visual (100 %)	
Right	−10.3	624	Superior Parietal (100 %)	LIPv (62.9 %)	Dorsal Attention (96.3 %)	
Right	−8.3	584	Superior Parietal (71.8 %)	IPS1 (41.9 %)	Visual (66.6 %)	
Left	−7.3	474	Superior Frontal (100 %)	8B (66.2 %)	Default (100 %)	
Right	−6.7	467	Middle Temporal (75.8 %)	TGd (74.1 %)	Default (72.6 %)	
Side	**Peak *T***	**Vol.** (mm^3)		**Peak Coordinates (MNI)**		**Brain Region**
			X	**Y**	**Z**	
Left	−8.6	9264	−28	−80	−32	Cerebellum
	−7.1		−30	−80	−38	
	−5.6		−14	−82	−32	
Right	−5.8	3272	20	−76	−36	Cerebellum
	−5.4		32	−84	−30	
	−5.3		26	−78	−32	
Right	−4.8	576	14	−4	18	Caudate
	−4.5		12	2	12	
	−4.4		12	−10	20	
Right	−4.9	400	10	−30	−2	Thalamus
	−4.1		18	−30	−2	
Left	−4.8	352	−8	−16	8	Thalamus
	−4.3		−12	−18	2	
Right	−4.7	328	12	−14	0	Thalamus
	−4.7		12	−14	8	
	−3.9		14	−22	−2	
Left	−4.8	232	−12	−22	−6	Thalamus
	−4.3		−16	−26	−8	
Left	−4.7	72	−20	−66	−54	Cerebellum
Bilat	−4.8	56	−2	−24	−46	Brainstem

Only the largest 10 clusters and parcellation labels are listed here.
[a] 5% threshold for positive activation *T*-value is 4.77.
[b] 5% threshold for negative activation *T*-value is −4.72.

2016). Our finding of reduced activation in many brain regions during reward attainment is less in line with previous literature. However, several fMRI studies have documented that reward prediction elicited stronger activation than reward attainment in the thalamus and midbrain (Haber and Knutson, 2010; Knutson and Greer, 2008). Similar findings were also documented in a recent fMRI study using the MID in 1,510 healthy adolescents, where reward expectancy reliably activated many typical reward areas (ventral striatum, pallidum, cingulate cortex, midbrain) as well as the thalamus, insula, hippocampus, motor cortex, and occipital areas, while reward attainment elicited much more limited activation (ventromedial prefrontal cortex, de-activation in the bilateral thalamus; Cao et al., 2019). Our findings are thus consistent with the notion that distinct reward processes entail coordination between different subsets of brain regions. Additionally, our secondary analyses revealed activation of the ventral striatum during receipt of unexpected rewards versus non-rewards. Previous studies have suggested a general role of the ventral striatum in both reward expectancy and attainment. Ventral striatum activation during attainment is usually linked to unexpected or uncertain rewards (Diekhof et al., 2012) or to early reward learning and initial positive feedback (Galvan et al., 2005). This preferential engagement by novel rewarding stimuli might account for the lack of ventral striatum activation in our contrast of certain reward vs non-reward attainment, as participants had a clear expectation of future outcome.

Interestingly, our secondary analyses indicated that reward attainment elicited not just reduced but directly opposite activation patterns

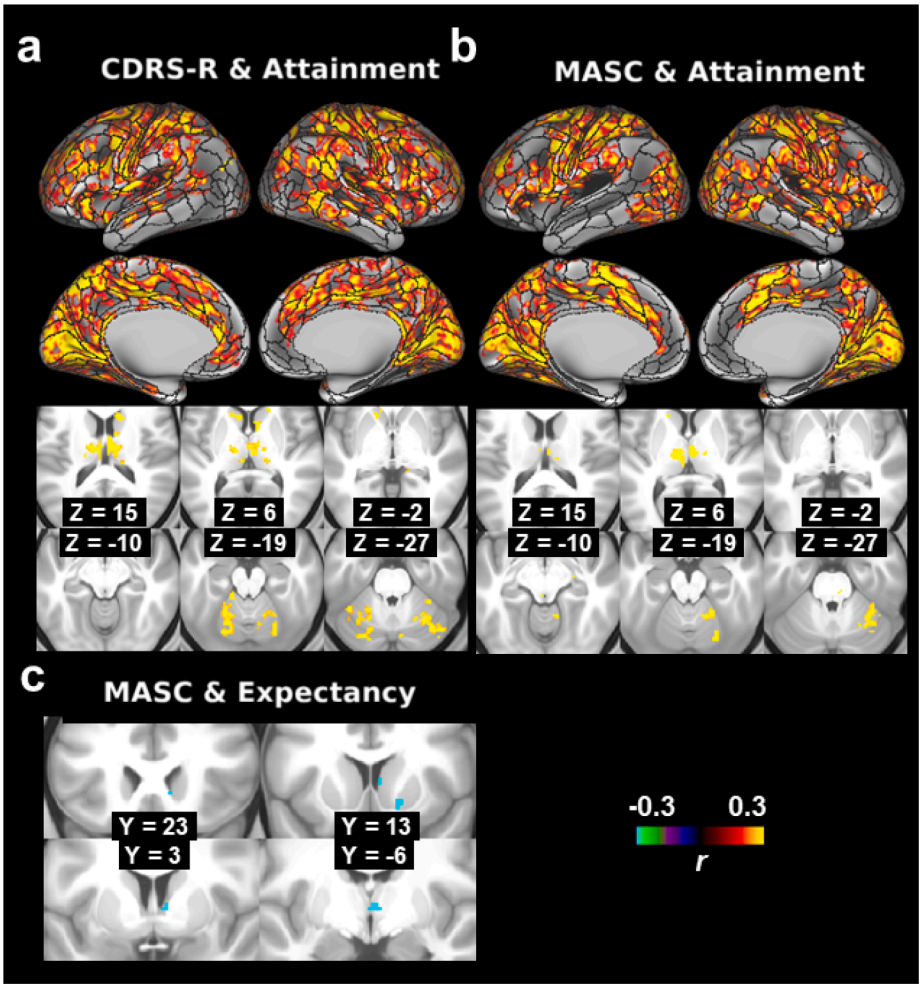

Fig. 3. Neural activation during reward attainment was positively associated with the severity of a) depression (CDRS-R) and b) anxiety (MASC) symptoms. c) Neural activation during reward expectancy was negatively associated with anxiety severity. Maps display Pearson's *r* values thresholded at $p_{TFCE\text{-}FWE} < 0.05$. The background overlay is mean sulcus depth from the HCP 1200 subject dataset. Black lines on the surface represent HCP MMP Atlas.

compared to reward expectancy across wide swaths of the cortex, with whole-brain cosine similarity significantly below zero for certain reward attainment. Cortical and subcortical brain regions play distinct roles in adolescent behaviors. The widely accepted "dual neural systems" model (Casey et al., 2008; Ernst et al., 2009) emphasizes a cortical cognitive regulatory system that is mainly supported by the prefrontal cortex and a subcortical emotional/motivational system that is mainly supported by the striatum and amygdala. Under this framework, our finding of widespread cortical deactivation during reward attainment might reflect reduced cognitive demands once expected rewarding outcomes are presented. A noteworthy exception to this general pattern was the visual cortex, where activation remained positive during reward attainment, albeit reduced in magnitude relative to expectancy. Integration between sensory and reward systems plays an important part in reward processing, with 55–70% of dopaminergic neurons activated by conditioned visual and/or auditory stimuli (Schultz, 1998). Recent work has highlighted the reciprocal nature of these interactions; one study in mice reported that neuronal activity in area V1 was more selective and reliable following visual stimuli associated with rewards vs neutral outcomes (Henschke et al., 2020). Moreover, our secondary analyses indicated that ventral striatum activation also remained significantly positive following uncertain reward attainment (**Fig. S7**). This result aligns with the well-established preclinical finding that dopaminergic responses to visual stimuli attenuate once stimulus-reward associations have been established, but are restored if reward outcomes become unpredictable (Schultz, 1998). As such, it is possible that the persistent coactivation of striatal and early visual regions we observed during uncertain reward attainment may reflect reinforcing feedback between the reward and visual systems to improve stimulus discrimination.

To examine how altered neural reward function contributes to psychiatric symptomatology in adolescents, we analyzed associations of activation during reward expectancy and attainment with dimensional measures of clinical symptom severity. Correlation analyses revealed that reduced basal ganglia and thalamus activation was specifically associated with anxiety rather than depression or anhedonia severity. This is consistent with our secondary group comparison results as well as previous *meta*-analyses and reviews (Keren et al., 2018; Toenders et al., 2019), which showed that adolescents with mood and anxiety symptoms exhibited blunted activation in the caudate and thalamus during reward expectancy compared to their healthy counterparts. Behaviorally, threat and anxiety inhibit reward-seeking behavior and *vice versa*. Similarly, our recent study found brain activation within the key salience and pain network regions during reward processes predicted worse depression outcomes in 2-year follow-up (Liu et al., 2020). These findings and our results suggest the importance of the negative valence system (NVS) function during reward motivation stage in early onset of mood and anxiety disorders.

In contrast to the limited associations with symptom severity detected for reward expectancy, neural activation during reward attainment was extensively correlated with depression and anxiety scores. These positive symptom correlations were found in multiple cortical and subcortical regions and substantially overlapped both with

Table 3
Associations between clinical symptoms and neural reward activation.

CDRS-R & Reward Attainment (RA) [a]

Side	Peak *r*	Area (mm^2)	Cluster Overlap: Desikan-Killiany Atlas (Desikan 2006)	HCP Atlas (Glasser 2016)	7-Network iFC Atlas (Yeo 2011)	
Right	0.49	1141	Lingual (38.1 %)	V1 (57.5 %)	Visual (99.1 %)	
Left	0.52	691	Peri-calcarine (53.5 %)	V1 (70.0 %)	Visual (100 %)	
Left	0.46	638	Lingual (83.9 %)	V1 (46.2 %)	Visual (100 %)	
Left	0.45	584	Precuneus (62.3 %)	7Pm (40.2 %)	Frontoparietal (45.9 %)	
Right	0.52	284	Inferior Parietal (62.8 %)	STV (50.3 %)	Default (63.0 %)	
Left	0.46	251	Cuneus (74.5 %)	V2 (54.8 %)	Visual (100 %)	
Right	0.45	247	Superior Parietal (52.5 %)	2 (92.3 %)	Somatomotor (52.6 %)	
Left	0.47	234	Lingual (96.3 %);	ProS (46.2 %)	Visual (100 %)	
Right	0.44	189	Superior Parietal (100 %)	POS2 (50.9 %)	Dorsal Attention (84.0 %)	
Right	0.46	187	Caudal Middle Frontal (52.1 %)	6a (94.2 %)	Dorsal Attention (78.9 %)	
Side	**Peak *r***	**Vol. (mm^3)**		**Peak Coordinates (MNI)**		**Brain Region**
			X	**Y**	**Z**	
Left	0.45	6072	−34	−46	−34	Cerebellum
	0.44		−18	−62	−16	
	0.41		−14	−38	−18	
Bilat	0.49	5896	4	−12	10	Thalamus; Caudate
	0.48		8	8	6	
	0.48		−16	−4	20	
Right	0.53	4416	30	−56	−30	Cerebellum
	0.47		36	−50	−36	
	0.46		28	−72	−20	
Right	0.42	2544	22	−70	−52	Cerebellum
	0.42		34	−70	−58	
	0.41		20	−64	−46	
Left	0.44	752	−8	14	6	Caudate
	0.40		−16	20	2	
	0.39		−14	16	−2	
Bilat	0.48	696	−10	−60	−42	Brainstem
	0.39		2	−50	−36	
	0.34		−6	−48	−36	
Bilat	0.43	328	4	−74	−34	Cerebellum
	0.36		−2	−72	−34	
	0.34		6	−80	−34	
Right	0.44	224	12	16	16	Caudate
Left	0.38	224	−40	−66	−56	Cerebellum
	0.35		−38	−60	−60	
Left	0.51	160	−24	−46	−56	Cerebellum
Right	0.39	120	20	20	10	Caudate
Right	0.43	112	10	−74	−26	Cerebellum
Left	0.40	96	−18	−42	−44	Cerebellum
Right	0.38	88	18	−74	–32	Cerebellum
Left	0.39	80	−14	−74	−46	Cerebellum
Left	0.39	48	−6	−56	−34	Cerebellum

MASC & Reward Expectancy (RE)

Side	Peak *r*	Vol. (mm^3)	Peak Coordinates (MNI)			Brain Region
			X	**Y**	**Z**	
Right	−0.48	480	4	−4	4	Thalamus; Caudate
	−0.41		8	8	6	
	−0.40		10	22	−2	
Right	−0.43	288	16	12	−8	Putamen
	−0.38		16	16	−4	
Left	−0.42	96	−6	−12	8	Thalamus
Left	−0.49	72	−18	8	−2	Putamen

MASC & RewardAttainment (RA) [b]

Side	Peak *r*	Area (mm^2)	Cluster Overlap: Desikan-Killiany Atlas (Desikan 2006)	HCP Atlas (Glasser 2016)	7-Network iFC Atlas (Yeo 2011)
Right	0.47	1638	Peri-calcarine (37.1%)	V1 (61.6%)	Visual (95.1%)
Left	0.48	1312	Peri-calcarine (38.3%)	V1 (73.3%)	Visual (99.8%)
Right	0.45	460	Fusiform (75.9%)	V4 (37.0%)	Visual (100%)
Right	0.46	365	Lingual (100%)	V2 (76.2%)	Visual (100%)
Left	0.43	330	Superior Frontal (57.2%)	6a (93.6%)	Dorsal Attention (75.3%)
Left	0.41	295	Superior Parietal (100%)	7PC (55.4%)	Dorsal Attention (58.1%)
Left	0.43	259	Pre-central (100%)	PEF (56.3%)	Dorsal Attention (69.7%)
Left	0.42	258	Pre-central (100%)	6d (100%)	Somatomotor (100%)
Right	0.44	234	Cuneus (96.1%)	V2 (77.7%); V3 (22.3%)	Visual (100%)
Right	0.45	220	Post-central (66.6%)	2 (87.4%)	Dorsal Attention (52.4%)

(*continued on next page*)

Table 3 (*continued*)

			MASC & RewardAttainment (RA) [b]			
Side	**Peak *r***	**Area (mm^2)**	**Cluster Overlap: Desikan-Killiany Atlas (Desikan 2006)**	**HCP Atlas (Glasser 2016)**	**7-Network iFC Atlas (Yeo 2011)**	
Side	**Peak *r***	**Vol. (mm^3)**	**Peak Coordinates (MNI)**			**Brain Region**
			X	**Y**	**Z**	
Right	0.48	2792	30	−56	−30	Cerebellum
	0.44		34	−48	−28	
	0.43		26	−68	−18	
Left	0.42	904	−6	−14	6	Thalamus
	0.40		−12	−18	6	
	0.36		−4	−24	8	
Right	0.41	600	4	−14	6	Thalamus
	0.37		14	−18	4	
	0.34		16	−14	8	
Bilat	0.50	352	12	−26	−38	Brainstem
Right	0.42	264	18	−74	−44	Cerebellum
	0.39		16	−68	−48	
	0.37		22	−72	−52	
Left	0.42	240	−4	−72	−40	Cerebellum
	0.38		−14	−76	−44	
Right	0.35	88	26	−56	−48	Cerebellum
Right	0.42	80	24	−42	−54	Cerebellum
Right	0.47	72	10	−18	16	Thalamus
Right	0.36	72	18	−52	−52	Cerebellum

Only the largest 10 clusters and parcellation labels are listed here.

[a] 5% threshold for positive association *r*-value is 0.317.

[b] 5% threshold for positive association *r*-value is 0.298.

each other and with the regions found to be deactivated in the main reward attainment contrast. Consistent with the RDoC framework adopted for this study, the remarkable similarity of our findings across depression and anxiety scales, as well as derived anhedonia scores in our secondary analyses, suggests that these dimensional assessments may be capturing a common component or components of reward dysfunction contributing to multiple symptoms. In line with this interpretation, the association between reward attainment activation and derived anhedonia scores in our secondary analysis became non-significant after controlling for depression severity, and the derived anhedonia score was highly correlated with overall depression severity (i.e. CDRS-R minus the anhedonia-related item, $r = 0.78$). While several additional anhedonia assessments (SHAPS, TEPS) were collected as part of this study, only the derived anhedonia score was significantly correlated with reward attainment activation. The negative findings for standard anhedonia scales are consistent with another dimensional study, which found that SHAPS scores were correlated with physical effort to gain reward and neural activity during effort to avoid aversion, but not with reward expectancy or attainment in a cohort of 84 adolescents (Rzepa and McCabe, 2019). These results underscore the need for narrowly defined measures of reward capacity and other relevant mental processes to disentangle the mechanisms contributing to highly comorbid psychiatric conditions in adolescents.

Finally, we found that the pattern of opposite neural activation between reward expectancy and attainment was weaker (less negative cosine similarity) as depression severity increased. Additional secondary analyses revealed that adolescents with mood and anxiety symptoms had less negative cosine similarity between these contrasts in than HCs. These findings align nicely with several previous reports; one study documented an inverse relationship between neural activation during reward expectancy and reward prediction errors in the right ventral striatum of healthy, but not depressed, individuals (Greenberg et al., 2015); another found hyper-activation during reward expectancy and hypo-activation during reward attainment in frontostriatal reward regions in adults with remitted major depression (Dichter et al., 2012). The association between less negative cosine similarity and depression severity suggests that impairments are present across multiple reward processing stages and wider brain regions, rather than a single stage or specific to canonical reward network, in adolescent depression.

Taken together, our clinical results suggest that adolescents with mood and anxiety symptoms exhibit altered neural function during reward expectancy and attainment. The interaction between multiple reward process stages appears to play important roles early in the course of psychiatric conditions. A systematic investigation into brain function and reward processes is needed to better understand the onset and prognosis of adolescent mood and anxiety conditions. Further studies may examine how reward processes predict future outcome, contribute to later onset psychiatric disorders, as well as are altered with multiple dimensional symptoms similarly and differentially.

Several limitations as well as strengths should be noted in this study. First, although we recruited a relatively large sample of psychotropic-medication-free adolescents ($N = 84$), the majority of participants presented with mood and/or anxiety symptoms, so the diversity of clinical profiles may be a concern. Conversely, however, the wide range of symptom severity in our sample enabled us to capture a large range of variation in reward function, increasing our power to detect effects in correlation analyses. Similarly, we included a subset of 17 HCs to ensure adequate sampling of participants with low mood and anxiety symptom severity; due to the limited size of this sample, group comparisons between clinical and HC adolescents should be considered exploratory. Additionally, although psychosis and substance use entail altered reward function, we excluded adolescents with psychosis due to concerns about low incidence and distinct etiology relative to our cohort, and we excluded adolescents with substance use to limit the impact of exogenous psychoactive drugs on neural function, similar to our rationale for excluding psychotropic medications. Another caveat was the relatively wide age range across adolescence (12–20 years old). However, all participants had already achieved the later stages of puberty (Tanner stage ≥ 4), limiting the contribution of hormonal effects on development. Correlation analyses also controlled for age as well as sex, further mitigating concern. Finally, we note that this study was based on high-resolution fMRI with HCP-like multiband imaging sequences. As has recently come to light, the use of multiband acceleration may reduce sensitivity to subcortical BOLD signals, with more severe reductions seen at higher acceleration factors (Srirangarajan et al., 2021). Although our study employed a relatively modest 5x acceleration factor compared to the 8x factor used by the HCP, our use of multiband acceleration may have decreased effect sizes in mesolimbic regions of interest for studying reward processes. At the same time, the high spatial and temporal resolution of our data allowed us to incorporate several advanced

processing techniques, including ICA-FIX denoising and MSMAll alignment. As detailed in Fig. S1, these techniques enabled us to achieve improved signal localization and sensitivity. Although the optimal trade-off between image acceleration and subcortical sensitivity is an open question, our results suggest that future fMRI studies in adolescents would likely benefit from the use of sophisticated preprocessing methods initially developed to study adult cohorts.

5. Conclusion

Our study examined neural function during discrete reward processing phases in a unique pediatric sample with diverse psychiatric profiles. We found that reward expectancy activated the cortical-basal ganglia reward network as well as visual and cognitive control regions while reward attainment deactivated many of these regions. Activation during reward attainment was reduced compared to activation during reward expectancy, driven mainly by neural responses to certain rather than uncertain reward attainment. Correlation analyses suggested that reduced activation in the striatum and thalamus during reward expectancy was associated with anxiety, while increased activation in myriad reward, cognitive control, sensory, and motor regions was linked to depression and anxiety severity. Future work should extend these findings by investigating additional neural processes such as interaction between expectancy and attainment, reward learning as well as loss/punishment in typical and atypical psychiatric development.

CRediT authorship contribution statement

Qi Liu: Data curation, Investigation, Software, Supervision , Validation, Visualization. **Benjamin A. Ely:** Data curation, Investigation, Software, Supervision, Validation. **Emily R. Stern:** Software. **Junqian Xu:** Software. **Joo-won Kim:** Software, Validation. **Danielle G. Pick:** Data curation, Validation. **Carmen M. Alonso:** Investigation. **Vilma Gabbay:** Formal analysis, Investigation, Resources, Supervision, Validation.

Declaration of Competing Interest

The authors declare that they have no known competing financial interests or personal relationships that could have appeared to influence the work reported in this paper.

Data availability

Data will be made available on request.

Acknowledgements

This study was supported by the National Institutes of Health (NIH) grants R01MH120601, R01MH126821, R01DA054885, R01MH128878, and R21MH121920 to VG (PI) and R21MH126501 to BE (PI). This work was also supported in part through the computational resources and staff expertise provided by the Icahn School of Medicine at Mount Sinai (ISMMS) Scientific Computing, with additional resource support provided by the ISMMS Brain Imaging Center.

Ethical statement

This study was approved by the Icahn School of Medicine at Mount Sinai Institutional Review Board and Albert Einstein College of Medicine Institutional Review Board. The written informed consent was obtained from participants age 18 and older. Those under the age of 18 provided signed assent, and a parent or legal guardian provided signed informed consent.

Appendix A. Supplementary data

Supplementary data to this article can be found online at https://doi.org/10.1016/j.nicl.2022.103258.

References

Beck, A.T., Steer, R., Brown, G., 1996. Beck depression inventory–second edition. The Psychological Corporation, Manual San Antonio, TX.
Bradley, K.A.L., Case, J.A.C., Freed, R.D., Stern, E.R., Gabbay, V., 2017. Neural correlates of RDoC reward constructs in adolescents with diverse psychiatric symptoms: a Reward Flanker Task pilot study. J. Affect. Disord. 216, 36–45.
Cao, Z., Bennett, M., Orr, C., Icke, I., Banaschewski, T., Barker, G.J., Bokde, A.L.W., Bromberg, U., Büchel, C., Quinlan, E.B., Desrivières, S., Flor, H., Frouin, V., Garavan, H., Gowland, P., Heinz, A., Ittermann, B., Martinot, J.-L., Nees, F., Orfanos, D.P., Paus, T., Poustka, L., Hohmann, S., Fröhner, J.H., Smolka, M.N., Walter, H., Schumann, G., Whelan, R., 2019. Mapping adolescent reward anticipation, receipt, and prediction error during the monetary incentive delay task. Hum. Brain Mapp. 40 (1), 262–283.
Casey, B.J., Getz, S., Galvan, A., 2008. The adolescent brain. Dev. Rev. 28 (1), 62–77.
Casey, B.J., Duhoux, S., Cohen, M.M., 2010. Adolescence: what do transmission, transition, and translation have to do with it? Neuron 67 (5), 749–760.
Costi, S., Morris, L.S., Collins, A., Fernandez, N.F., Patel, M., Xie, H., Kim-Schulze, S., Stern, E.R., Collins, K.A., Cathomas, F., Parides, M.K., Whitton, A.E., Pizzagalli, D.A., Russo, S.J., Murrough, J.W., 2021a. Peripheral immune cell reactivity and neural response to reward in patients with depression and anhedonia. Transl. Psychiatry 11 (1).
Costi, S., Morris, L.S., Kirkwood, K.A., Hoch, M., Corniquel, M., Vo-Le, B., Iqbal, T., Chadha, N., Pizzagalli, D.A., Whitton, A., Bevilacqua, L., Jha, M.K., Ursu, S., Swann, A.C., Collins, K.A., Salas, R., Bagiella, E., Parides, M.K., Stern, E.R., Iosifescu, D.V., Han, M.-H., Mathew, S.J., Murrough, J.W., 2021b. Impact of the KCNQ2/3 channel opener ezogabine on reward circuit activity and clinical symptoms in depression: results from a randomized controlled trial. Am. J. Psychiatry 178 (5), 437–446.
Cox, R.W., Chen, G., Glen, D.R., Reynolds, R.C., Taylor, P.A., 2017a. fMRI clustering and false-positive rates. PNAS 114, E3370–E3371.
Cox, R.W., Chen, G., Glen, D.R., Reynolds, R.C., Taylor, P.A., 2017b. fMRI clustering in AFNI: false-positive rates redux. Brain Connect. 7 (3), 152–171.
Crews, F., He, J., Hodge, C., 2007. Adolescent cortical development: a critical period of vulnerability for addiction. Pharmacol. Biochem. Behav. 86 (2), 189–199.
Desikan, R.S., Ségonne, F., Fischl, B., Quinn, B.T., Dickerson, B.C., Blacker, D., Buckner, R.L., Dale, A.M., Maguire, R.P., Hyman, B.T., Albert, M.S., Killiany, R.J., 2006. An automated labeling system for subdividing the human cerebral cortex on MRI scans into gyral based regions of interest. NeuroImage 31 (3), 968–980.
Dichter, G.S., Kozink, R.V., McClernon, F.J., Smoski, M.J., 2012. Remitted major depression is characterized by reward network hyperactivation during reward anticipation and hypoactivation during reward outcomes. J. Affect. Disord. 136 (3), 1126–1134.
Dickie, E.W., Anticevic, A., Smith, D.E., Coalson, T.S., Manogaran, M., Calarco, N., Viviano, J.D., Glasser, M.F., Van Essen, D.C., Voineskos, A.N., 2019. Ciftify: a framework for surface-based analysis of legacy MR acquisitions. NeuroImage 197, 818–826.
Diekhof, E.K., Kaps, L., Falkai, P., Gruber, O., 2012. The role of the human ventral striatum and the medial orbitofrontal cortex in the representation of reward magnitude – an activation likelihood estimation meta-analysis of neuroimaging studies of passive reward expectancy and outcome processing. Neuropsychologia 50 (7), 1252–1266.
Ding, Y.-D., Chen, X., Chen, Z.-B., Li, L.e., Li, X.-Y., Castellanos, F.X., Bai, T.-J., Bo, Q.-J., Cao, J., Chang, Z.-K., Chen, G.-M., Chen, N.-X., Chen, W., Cheng, C., Cheng, Y.-Q., Cui, X.-L., Duan, J., Fang, Y.-R., Gong, Q.-Y., Hou, Z.-H., Hu, L., Kuang, L.i., Li, F., Li, H.-X., Li, K.-M., Li, T., Liu, Y.-S., Liu, Z.-N., Long, Y.-C., Lu, B., Luo, Q.-H., Meng, H.-Q., Peng, D.-H., Qiu, H.-T., Qiu, J., Shen, Y.-D., Shi, Y.-S., Si, T.-M., Tang, Y.-Q., Wang, C.-Y., Wang, F., Wang, K., Wang, L.i., Wang, X., Wang, Y., Wang, Y.-W., Wu, X.-P., Wu, X.-R., Xie, C.-M., Xie, G.-R., Xie, H.-Y., Xie, P., Xu, X.-F., Yang, H., Yang, J., Yao, J.-S., Yao, S.-Q., Yin, Y.-Y., Yuan, Y.-G., Zang, Y.-F., Zhang, A.-X., Zhang, H., Zhang, K.-R., Zhang, L., Zhang, Z.-J., Zhao, J.-P., Zhou, R.-B., Zhou, Y.-T., Zhu, J.-J., Zhu, Z.-C., Zou, C.-J., Zuo, X.-N., Yan, C.-G., Guo, W.-B., 2022. Reduced nucleus accumbens functional connectivity in reward network and default mode network in patients with recurrent major depressive disorder. Transl. Psychiatry 12 (1).
Eklund, A., Nichols, T.E., Knutsson, H., 2016. Cluster failure: why fMRI inferences for spatial extent have inflated false-positive rates. PNAS 113 (28), 7900–7905.
Eklund, A., Knutsson, H., Nichols, T.E., 2019. Cluster failure revisited: impact of first level design and physiological noise on cluster false positive rates. Hum. Brain Mapp. 40 (7), 2017–2032.
Eriksen, B.A., Eriksen, C.W., 1974. Effects of noise letters upon the identification of a target letter in a nonsearch task. Percept Psychophys 16 (1), 143–149.
Ernst, M., Romeo, R.D., Andersen, S.L., 2009. Neurobiology of the development of motivated behaviors in adolescence: a window into a neural systems model. Pharmacol. Biochem. Behav. 93 (3), 199–211.
Fairchild, G., 2011. The developmental psychopathology of motivation in adolescence. Dev Cogn Neurosci 1 (4), 414–429.
Forbes, E.E., Dahl, R.E., 2012. Research review: altered reward function in adolescent depression: what, when and how? J. Child Psychol. Psychiatry 53, 3–15.

Galvan, A., Hare, T.A., Davidson, M., Spicer, J., Glover, G., Casey, B.J., 2005. The role of ventral frontostriatal circuitry in reward-based learning in humans. J. Neurosci. 25, 8650–8656.
Gard, D.E., Gard, M.G., Kring, A.M., John, O.P., 2006. Anticipatory and consummatory components of the experience of pleasure: a scale development study. J. Res. Pers. 40 (6), 1086–1102.
Glasser, M.F., Sotiropoulos, S.N., Wilson, J.A., Coalson, T.S., Fischl, B., Andersson, J.L., Xu, J., Jbabdi, S., Webster, M., Polimeni, J.R., Van Essen, D.C., Jenkinson, M., 2013. The minimal preprocessing pipelines for the Human Connectome Project. NeuroImage 80, 105–124.
Glasser, M.F., Coalson, T.S., Robinson, E.C., Hacker, C.D., Harwell, J., Yacoub, E., Ugurbil, K., Andersson, J., Beckmann, C.F., Jenkinson, M., Smith, S.M., Van Essen, D. C., 2016. A multi-modal parcellation of human cerebral cortex. Nature 536 (7615), 171–178.
Glasser, M.F., Coalson, T.S., Bijsterbosch, J.D., Harrison, S.J., Harms, M.P., Anticevic, A., Van Essen, D.C., Smith, S.M., 2018. Using temporal ICA to selectively remove global noise while preserving global signal in functional MRI data. NeuroImage 181, 692–717.
Greenberg, T., Chase, H.W., Almeida, J.R., Stiffler, R., Zevallos, C.R., Aslam, H.A., Deckersbach, T., Weyandt, S., Cooper, C., Toups, M., Carmody, T., Kurian, B., Peltier, S., Adams, P., McInnis, M.G., Oquendo, M.A., McGrath, P.J., Fava, M., Weissman, M., Parsey, R., Trivedi, M.H., Phillips, M.L., 2015. Moderation of the relationship between reward expectancy and Prediction error-related ventral striatal reactivity by anhedonia in unmedicated major depressive disorder: findings from the EMBARC study. Am. J. Psychiatry 172 (9), 881–891.
Griffanti, L., Salimi-Khorshidi, G., Beckmann, C.F., Auerbach, E.J., Douaud, G., Sexton, C. E., Zsoldos, E., Ebmeier, K.P., Filippini, N., Mackay, C.E., Moeller, S., Xu, J., Yacoub, E., Baselli, G., Ugurbil, K., Miller, K.L., Smith, S.M., 2014. ICA-based artefact removal and accelerated fMRI acquisition for improved resting state network imaging. NeuroImage 95, 232–247.
Haber, S.N., Knutson, B., 2010. The reward circuit: linking primate anatomy and human imaging. Neuropsychopharmacol 35 (1), 4–26.
Harms, M.P., Somerville, L.H., Ances, B.M., Andersson, J., Barch, D.M., Bastiani, M., Bookheimer, S.Y., Brown, T.B., Buckner, R.L., Burgess, G.C., Coalson, T.S., Chappell, M.A., Dapretto, M., Douaud, G., Fischl, B., Glasser, M.F., Greve, D.N., Hodge, C., Jamison, K.W., Jbabdi, S., Kandala, S., Li, X., Mair, R.W., Mangia, S., Marcus, D., Mascali, D., Moeller, S., Nichols, T.E., Robinson, E.C., Salat, D.H., Smith, S.M., Sotiropoulos, S.N., Terpstra, M., Thomas, K.M., Tisdall, M.D., Ugurbil, K., van der Kouwe, A., Woods, R.P., Zöllei, L., Van Essen, D.C., Yacoub, E., 2018. Extending the Human Connectome Project across ages: imaging protocols for the Lifespan Development and Aging projects. NeuroImage 183, 972–984.
Henschke, J.U., Dylda, E., Katsanevaki, D., Dupuy, N., Currie, S.P., Amvrosiadis, T., Pakan, J.M.P., Rochefort, N.L., 2020. Reward association enhances stimulus-specific representations in primary visual cortex. Curr. Biol. 30 (10).
Kaufman, A.S. (1990). Kaufman brief intelligence test: KBIT (AGS, American Guidance Service Circle Pines, MN).
Kaufman, JOAN, Birmaher, BORIS, Brent, DAVID, Rao, UMA, Flynn, CYNTHIA, Moreci, PAULA, Williamson, DOUGLAS, Ryan, NEAL, 1997. Schedule for Affective Disorders and Schizophrenia for School-Age Children-Present and Lifetime Version (K-SADS-PL): initial reliability and validity data. J Am Acad Child Adol Psychiatry 36 (7), 980–988.
Keren, H., O'Callaghan, G., Vidal-Ribas, P., Buzzell, G.A., Brotman, M.A., Leibenluft, E., Pan, P.M., Meffert, L., Kaiser, A., Wolke, S., Pine, D.S., Stringaris, A., 2018. Reward processing in depression: a conceptual and meta-analytic review across fMRI and EEG studies. Am. J. Psychiatry 175 (11), 1111–1120.
Knutson, B., Greer, S.M., 2008. Anticipatory affect: neural correlates and consequences for choice. Philos. Trans. R. Soc. Lond. B Biol. Sci. 363 (1511), 3771–3786.
Knutson, B., Westdorp, A., Kaiser, E., Hommer, D., 2000. fMRI visualization of brain activity during a Monetary Incentive Delay task. NeuroImage 12 (1), 20–27.
Liu, Q., Ely, B.A., Schwartz, J.J., Alonso, C.M., Stern, E.R., Gabbay, V., 2020. Reward function as an outcome predictor in youth with mood and anxiety symptoms. J. Affect. Disord. 278, 433–442.
March, J.S., Parker, J.D.A., Sullivan, KEVIN, Stallings, PATRICIA, Conners, C.K., 1997. The Multidimensional Anxiety Scale for Children (MASC): factor structure, reliability, and validity. J. Am. Acad. Child Adol Psychiatry 36 (4), 554–565.
Morris, L.S., Costi, S., Tan, A., Stern, E.R., Charney, D.S., Murrough, J.W., 2020. Ketamine normalizes subgenual cingulate cortex hyper-activity in depression. Neuropsychopharmacol 45 (6), 975–981.
Paus, T., 2005. Mapping brain maturation and cognitive development during adolescence. Trends Cogn Sci 9 (2), 60–68.
Poznanski, E.O., Freeman, L.N., Mokros, H.B., 1985. Children's Depression Rating Scale-Revised. Psychopharmacol. Bull. 21, 979–989.
Robinson, E.C., Jbabdi, S., Glasser, M.F., Andersson, J., Burgess, G.C., Harms, M.P., Smith, S.M., Van Essen, D.C., Jenkinson, M., 2014. MSM: a new flexible framework for Multimodal Surface Matching. NeuroImage 100, 414–426.
Rzepa, E., McCabe, C., 2019. Dimensional anhedonia and the adolescent brain: reward and aversion anticipation, effort and consummation. BJPsych Open 5 e99-e99.
Salimi-Khorshidi, G., Douaud, G., Beckmann, C.F., Glasser, M.F., Griffanti, L., Smith, S. M., 2014. Automatic denoising of functional MRI data: combining independent component analysis and hierarchical fusion of classifiers. NeuroImage 90, 449–468.
Schultz, W., 1998. Predictive reward signal of dopamine neurons. J. Neurophysiol. 80 (1), 1–27.
Sequeira, S.L., Forbes, E.E., Hanson, J.L., Silk, J.S., 2022. Positive valence systems in youth anxiety development: a scoping review. J. Anxiety Disord. 89.
Silverman, M.H., Jedd, K., Luciana, M., 2015. Neural networks involved in adolescent reward processing: an activation likelihood estimation meta-analysis of functional neuroimaging studies. NeuroImage 122, 427–439.
Snaith, R.P., Hamilton, M., Morley, S., Humayan, A., Hargreaves, D., Trigwell, P., 1995. A scale for the assessment of hedonic tone: the Snaith-Hamilton Pleasure Scale. Br. J. Psychiatry 167 (1), 99–103.
Srirangarajan, T., Mortazavi, L., Bortolini, T., Moll, J., Knutson, B., 2021. Multi-band fMRI compromises detection of mesolimbic reward responses. NeuroImage 244.
Stern, E.R., Welsh, R.C., Fitzgerald, K.D., Gehring, W.J., Lister, J.J., Himle, J.A., Abelson, J.L., Taylor, S.F., 2011. Hyperactive error responses and altered connectivity in ventromedial and frontoinsular cortices in obsessive-compulsive disorder. Biol. Psychiatry 69 (6), 583–591.
Taylor, S.F., Martis, B., Fitzgerald, K.D., Welsh, R.C., Abelson, J.L., Liberzon, I., Himle, J. A., Gehring, W.J., 2006. Medial frontal cortex activity and loss-related responses to errors. J. Neurosci. 26, 4063.
Thomas Yeo, B.T., Krienen, F.M., Sepulcre, J., Sabuncu, M.R., Lashkari, D., Hollinshead, M., Roffman, J.L., Smoller, J.W., Zöllei, L., Polimeni, J.R., Fischl, B., Liu, H., Buckner, R.L., 2011. The organization of the human cerebral cortex estimated by intrinsic functional connectivity. J. Neurophysiol. 106 (3), 1125–1165.
Toenders, Y.J., van Velzen, L.S., Heideman, I.Z., Harrison, B.J., Davey, C.G., Schmaal, L., 2019. Neuroimaging predictors of onset and course of depression in childhood and adolescence: a systematic review of longitudinal studies. Dev Cogn Neurosci 39.
Wang, K.S., Smith, D.V., Delgado, M.R., 2016. Using fMRI to study reward processing in humans: past, present, and future. J. Neurophysiol. 115 (3), 1664–1678.
Winkler, A.M., Ridgway, G.R., Webster, M.A., Smith, S.M., Nichols, T.E., 2014. Permutation inference for the general linear model. NeuroImage 92, 381–397.
Winkler, A.M., Webster, M.A., Brooks, J.C., Tracey, I., Smith, S.M., Nichols, T.E., 2016. Non-parametric combination and related permutation tests for neuroimaging. Hum. Brain Mapp. 37 (4), 1486–1511.